



# Lightweight Deep Reinforcement Learning Model for Energy-Efficient Resource Allocation in Edge Computing

Ghassan A. Abed<sup>1,\*</sup>, , Mohanad A. Al-askari<sup>2</sup>, 

<sup>1</sup> Network & Cybersecurity Engineering Department, College of Engineering, Al-Iraqia University, Iraq

<sup>2</sup> Biomedical Engineering Research Centre, University of Anbar, Ramadi 31001, Anbar, Iraq

## ARTICLEINFO

### Article History

Received 07 Aug 2025  
Revised 08 Sep 2025  
Accepted 04 Oct 2025  
Published 07 Oct 2025

### Keywords

Digital twin  
6G networks  
Infrastructure planning,  
Extended reality  
XR



## ABSTRACT

A lightweight digital twin model for a single 6G cell operating in the D-band (140 GHz) with a 1 GHz bandwidth is presented in this work with the goal of assessing the cell's capacity, coverage, and terminal time in order to support extended reality (XR) applications. With a tangent dispersion of 3 dB and a path exponent of  $n = 2.2$ , the model is based on the free-space loss equation as per ITU-R Recommendation P.525. The instantaneous capacity is determined using the Shannon-Hartley theorem. Three XR sessions are created every minute using a Poisson method, and their durations are determined by an exponential distribution (mean of 120 seconds). In accordance with 3 GPP and Ericsson guidelines for normal XR loads, the bit needs per user are randomly selected to fall between 40 and 120 Mb/s. The average coverage was around 92 %, the average cell capacity was approximately 5.1 Gb/s, and the edge capacity (lowest quintile) was approximately 230 Mb/s, according to fifty statistical forecasts. Additionally, the 95th percentile round-trip latency was 3.9 ms, which is significantly less than the permitted maximum (10–20 ms) for immersive XR research. These findings suggest that modest XR loads may be supported by a 250-meter cell with a high-gain antenna layout without the need to immediately lower the radius or raise the transmitted power. However, the model remains theoretical and simplified, excluding geometric blockage and cell overlap in complex metropolitan environments.

## 1. INTRODUCTION

Digital twins (DT) are precise, multi-level digital replicas of real-world items. These entities may include complex physical systems such as machinery, robots, industrial processes, or electronic devices [1]. A virtual model, associated operating data, and analysis tools make up a digital twin in the virtual realm [2], as shown in Figure 1.

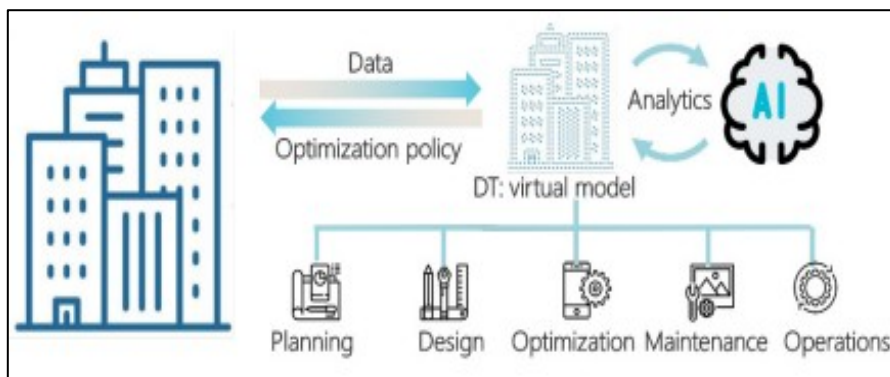


Fig. 1. The digital twin model [3].

There is a reciprocal relationship between digital and real-world objects: In order to create DT models, physical systems transmit real-time data to the virtual environment. DT then evaluate the data they have gathered, update the models, and provide the physical items optimization rules to enhance their functionality [4]. As shown in Figure 2., a whole DT model is made up of three parts: data, model, and software.

\*Corresponding author. Email: [ghassan.a.abed@aliraqia.edu.iq](mailto:ghassan.a.abed@aliraqia.edu.iq)

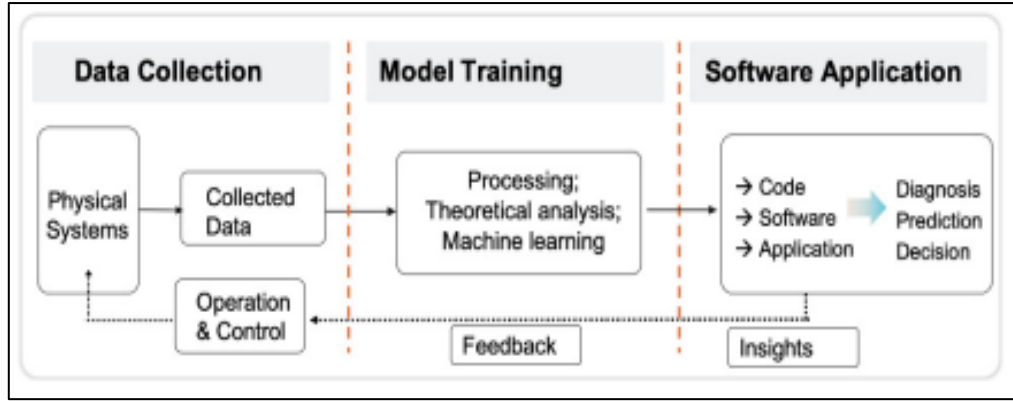


Fig. 2. Digital twin- data model software [4].

Applications for augmented reality (XR) need end-to-end latency of less than 20 milliseconds and data speeds of up to several gigabits. These criteria can be met by sixth generation (6G) networks that operate in the sub-terahertz (sub-terahertz) frequency band. Network planners may assess performance before implementation thanks to the digital twin, which lowers risk and expenses [5].

6G has substantial prospects, notwithstanding constraints like as spectrum management, energy efficiency, and hardware integration [6].

In this study, we provide a novel extended reality function (XRF) model. This concept deploys a digital twin network (DTN) by utilising DT technology.

The original network, which may be a real or virtual network, is replicated in the DTN. Through new immersive network features including resource finder, intelligent monitoring, critical node detection, interactive network status visualisations, and optimised routing, the XRF module is intended to improve the network experience. This network needs a supporting architectural framework to be deployed more easily [7]. To guarantee appropriate twinning, synchronisation, and self-management for the deployment of the DTN and the XRF-enabled module, the supporting architecture needs to be strong and dependable [8].

Mobile devices, such as laptops, tablets, and smartphones, are categorised as digital twin client devices (DTCDs) as the DTN and XRF networks are intended to be an improved, portable version of the digital twin of the original network [9]. The suggested architectural framework simulates XR traffic (Poisson arrivals and exponential time frames), builds a digital twin of a central 6G cell, and determines the link budget using a Log-Distance attenuation model (with shadow fading), as DTCDs generally lack sophisticated computer units [10].

It is crucial to stress that the suggested smart network makes it possible to access a duplicate of any network that is linked to the Internet, complete with all of its resources and services [11]. However, the idea of Network as a Service (NaaS) is not in line with this approach [12]. Instead of being owned by a third party, the present idea replicates the original network where XR services are implemented [13].

## 2. LITERATURE REVIEW

Numerous survey studies about the use of DT technology in different manufacturing, industrial, and service applications have been published.

Virtual/augmented reality (VR/XR), remote surgery, autonomous vehicles, and instant holographic communications are just a few of the applications that are becoming more and more popular as a result of the rapid advancement of technology. These applications all require high transmission rates and ultra-low latency in 6G and beyond (6G+) networks. This makes it extremely difficult to implement large-scale networks effectively while maintaining user experience in areas like network design, planning, troubleshooting, optimisation, and maintenance. The development of a virtual model that replicates the real network, allowing for the simulation of various network architectures, the implementation of various operating policies, and the replication of intricate failure scenarios under realistic circumstances, has made network digital twin (NDT) technology a promising remedy. This is the driving force behind this study, in which we provide an extensive overview of non-destructive testing in the context of 6G+, touching on topics like cloud/edge computing, applications (blockchain, healthcare, manufacturing, security, vehicular networks), non-terrestrial networks (NTNs), quantum networks, and radio access networks (RAN) from both academic and industrial viewpoints [14]. A thorough architectural framework is presented in the paper by Calle-Heredia and Hesselbach to facilitate the deployment of XR functions (XRFs) in a digital twin network

(DTN) environment. This framework allows for the provision of immersive functionality, such as control and management functions, that are not available in the native network. With the help of a network topology configuration and the requirement for minimal hardware and software resources, the suggested architecture offers a strong and portable framework that enables devices with low processing power, like laptops and smartphones, to take advantage of the DTN's improved network functionality without affecting the native network (ON) [15].

The goal of the study Yang et al. presented was to create a technical framework that would increase the usability of XR-based HMI systems and the efficiency of XR application development. The four-layer framework they initially presented included a perception layer that included a real machine and a simulation model based on a robot operating system, a machine communication layer, a network layer that included three different kinds of communication middleware, and a service layer built with Unity that produced digital applications based on XR. They went on to evaluate the framework's responsiveness and outline a number of XR-based industrial uses for a DT-based smart crane [16].

Recently, QUIC, a new transport protocol, was launched as a TCP substitute to enhance the performance of mobile web services. It is challenging to decide whether and when to employ QUIC in large-scale mobile web services, nevertheless, considering its benefits and drawbacks. The choice of transport protocols is influenced by a number of factors, including the restricted diversity of QUIC implementations, the high user variability in statewide deployments, the complicated temporal correlation of network circumstances, and the resources available on mobile devices. In order to improve web request completion time and transition between transport protocols for online mobile web services, Zhang et al. introduce WiseTrans, an adaptive transport protocol selection technique, in their study. In order to achieve high performance at a reasonable operating cost, WiseTrans employs machine learning techniques to address temporal variability, makes decisions based on historical data to address spatial variability, uses an online learning approach to address implementation variability, and switches transport protocols at the request level. We integrate WiseTrans into Baidu's well-known mobile web services app on both the iOS and Android operating systems. Extensive tests shown that, on average, WiseTrans may cut order completion times by up to 25.8% when compared to a single procedure [17].

### 3. SIXTH-GENERATION (6G) NETWORKS

By 2030, Sixth-generation (6G) networks—the logical next step in wireless technology—should be available. With a reaction time of under a thousandth of a second, they may achieve connection rates of up to terabits per second. Additionally, artificial intelligence will be immediately integrated into these networks, improving the intelligence and efficiency of communications [18].

6G networks promise exceptional capabilities that go beyond what we now understand about communications thanks to a number of aspects that make them a significant advancement over fifth-generation (5G) networks. First off, 6G networks are predicted to achieve previously unheard-of speeds of terabits per second, which would enable the transport of enormous volumes of data in a matter of milliseconds. Users will be able to operate large apps that need immediate data processing, including deep learning and artificial intelligence, or download HD movies in a matter of seconds thanks to these incredibly fast speeds [19].

Almost instantaneous communications are made possible by 6G networks' ultra-low latency, which is just milliseconds. For time-sensitive applications, like remote surgery that necessitates great accuracy and prompt command execution, or self-driving cars that depend on real-time choices to prevent accidents, this advancement is perfect. Additionally, interactive gaming and virtual reality apps will be transformed by this ultra-responsiveness, which will enhance the realism and smoothness of experiences [20].

The enormous ability of 6G networks to link a large number of devices at once is another crucial feature. These networks will serve as the backbone of smart cities as the Internet of Things (IoT) grows, allowing for the integration of smart infrastructure, household appliances, and traffic lights. In addition to improving service efficiency, this pervasive connection will make daily life smarter and more convenient [21].

The incorporation of artificial intelligence into the architecture of 6G is another unique characteristic. These networks will develop into intelligent systems that can learn and perform better than only serving as a channel for data transmission. Through the analysis of real-time data, networks will be able to better manage energy use and tailor their services to each user's demands [22].

Lastly, terahertz frequencies, which offer a large bandwidth that permits data transfer at tremendous speeds, are the foundation of 6G networks. Although using these high frequencies presents certain difficulties, such as the requirement to create new technologies to address signal loss, they can lead to whole new uses, such as sophisticated sensor systems and high-quality satellite communications [23].

#### 4. EXTENDED REALITY (XR)

In addition to being a general word for augmented reality (AR), mixed reality (MR), and virtual reality (VR), extended reality (XR) also refers to and interpolates beyond these, enabling us to view radio waves, sound waves, and other unseen phenomena. Users will be immersed in a virtual or augmented environment as a result of the technology's ability to mix or mirror the real world with a "digital twin world" that can interact with it [24].

Beyond academic fields, extended reality is expanding quickly and is now having practical applications in a variety of industries, including entertainment, film, marketing, real estate, manufacturing, education and maintenance, and teleworking. It is also having an impact on the real world in the fields of medicine, architecture, education, and industry. The potential for shared usage in training, education, treatments, the workplace, and data exploration and analysis are what define extended reality [25].

The way extended reality works is by gathering visual information that may be shared or seen locally, then sending it to human senses over a network. These gadgets allow for instantaneous reactions in a virtual stimuli, resulting in customised experiences [26].

5G technology advancements and edge computing, or processing that takes place "at or near the data source," can assist boost user capacity, lower latency, and improve data rates. The future of extended reality is probably going to grow as a result of these uses [27].

In order to increase an object's (human or technical) sensory capacity by immersing it in a closed feedback loop, extended reality may be used to both humans and technology as entities. We refer to this kind of expanded intelligence as veil metrics [28].

#### 5. METHODOLOGY

To swiftly confirm a 6G cell's capacity, latency, and coverage for XR sessions, the application builds a lightweight digital twin of the cell running at 140 GHz. Fifty statistical drops are used to do this, with each drop varying in terms of user locations and distracting situations. MATLAB 2021b was used to simulate and develop the suggested system.

An algorithm called Deep Q-Network (DQN) is used. While networks like those used in PPO or A3C have low computation and memory needs, DQN employs a massive neural network. In addition to parallel or execution updates, Q-value updates are based on classical Q-learning, which uses less resources by updating advise one experiment at a time (using an experiment replay buffer). Because DQN relies on direct performance optimisation (policy-based) rather than value estimation (value-based), it is more challenging to compare with algorithms like PPO that also depend on direct performance optimisation. It is a specialised tool that improves privacy and language customisation by reducing the size of the network or the number of computer environments on both sides with restricted resources. For grid or cyber computing applications that need highly effective reinforcement learning models with low resource usage, DQN is appropriate.

##### 5.1 Physical Layer Parameters

Computer bits are sent from one device to another across the network by the physical layer. Its responsibilities include deciding how the network's physical connections are established and how bits are converted into recognisable signals for transmission via radio waves, optical, or electrical means.

TABLE I. PHYSICAL LAYER PARAMETERS

Symbol	Physical meaning	Typical values / range (for 6G @ 140 GHz)	Why it matters?
$f_c$	Carrier frequency	100 – 150 GHz (this work uses 140 GHz)	Higher $f_c \Rightarrow$ shorter wavelength (smaller antennas) and wider contiguous spectrum, but free-space loss and atmospheric absorption rise rapidly.
B	RF bandwidth	0.5 – 2 GHz contiguous blocks; we assume 1 GHz	Shannon capacity grows linearly with B; however $k_{TB}$ noise power also scales with B.
$P_t$	Transmit power (gNB)	24 – 33 dBm EIRP for sub-THz test chips; we use 30 dBm	Regulated by safety limits; every +3 dB gains $\approx 12\%$ cell-radius increase when $n \approx 2.2$ .
$G_b, G_r$	Antenna gain (Tx/Rx arrays)	28 – 32 dBi at gNB (256-element phased arrays); 10–15 dBi at UE	High gain beams offset the large path loss and suppress interference; requires fast beam-tracking.
NF	Receiver noise figure	6 – 10 dB for CMOS/SiGe D-band LNAs; we assume 7 dB	Lower NFNF directly improves link budget and cell radius; challenging at 140 GHz due to device noise [29].
$N_0$	Wideband noise power	$N_0 [\text{dBm}] = k_t + 10 \log_{10} B + NF \rightarrow -83 \text{ dBm at } 1 \text{ GHz \& } 7 \text{ dB NFNF}$	Sets SNR floor; every +3 dB increase halves capacity for fixed $P_r$ . (Formula from thermal-noise standard)
$\lambda$	Wavelength	$\lambda = c/f_c \approx 2.1 \text{ mm at } 140 \text{ GHz}$	Enters FSPL; doubling $f_c$ raises FSPL by 6 dB for equal distance.

$N_n$	Path-loss exponent	2.0 (LoS) – 2.4 (urban micro-cells); we use 2.2	Captures scattering & blockage beyond free space; governs how fast signal decays with distance.
$\sigma_{\text{shadow}}$	Shadow-fading stdev	2 – 4 dB indoor; 3 – 6 dB outdoor; we use 3 dB	Models large-scale shadowing; drives outage probability & coverage margin.
$\gamma_a$	Atmospheric attenuation	< 1 dB / km near 140 GHz (dry air); peaks at specific absorption lines	Matters for backhaul & long ranges; negligible below 0.5 km but dominates links $\geq 1$ km.

All numerical options follow the recent sub-THZ channel and prototype chip results. There are basic relations used in the research:

$$\text{Free – space path loss (FSPL)} = 20 \log_{10} \left( \frac{4\pi d}{\lambda} \right) \quad (1)$$

$$\text{Wideband capacity: } C = B \log_2 (1 + \text{SNR}) \quad (2)$$

## 5.2 Signal path model

The free space model is used with a path exponent of  $n=2.2$  and Gaussian tangent scattering:

$$\text{PL}(d) = 20 \log_{10} \left( \frac{4\pi d}{\lambda} \right) + 10 n \log_{10} d + X_\sigma + \gamma_a d \quad (3)$$

FSPL dominates when  $d < 50$

The term  $10 n \log_{10} d$  captures additional loss from reflections and partial obstructions. The atmospheric-attenuation term  $\gamma_a d$  becomes significant only at long distances or high humidity.

## 5.3 Antenna Gain and Beam Enablement

To maintain high link speeds above 100 m, 6G uses  $16 \times 16$  element arrays (256 antennas) that yield  $\approx 31$  dBi. Doubling the number of elements increases gain by +3 dB, but increases power consumption and the algorithms required to track the moving device.

## 5.4 Capacity (Shannon–Hartley theorem)

An upper limit on a link's capacity, expressed in bits per second (bps), is provided by Shannon's Theorem and depends on the available bandwidth and the link's signal-to-noise ratio.

The Theorem may be expressed as follows:

$$C = B \log_2 (1 + \text{SNR}_{iln}) \left[ \frac{\text{bit}}{\text{s}} \right] \quad (4)$$

where B is the line's bandwidth and C is the possible channel capacity.

## 5.5 Wideband and Channel Coding

With  $B=1$  GHz; even in 64-QAM (six bits/symbol) mode and  $\text{SNR}=25$  dB can be achieved.

$$R = \eta_{SE} B = \frac{6 \frac{\text{bit}}{\text{s}}}{\text{Hz}} \times 1 \text{GHz} = 6 \text{Gb/s} \quad (5)$$

With dual-polarized antennas ( $2 \times 2$  MIMO) the theoretical rate is doubled to 12 Gb/s if minimal interference is achieved.

## 5.6 Physical delay (latency)

Bidirectional propagation time:

$$T_{prop} = 2 \frac{d}{c} \approx 0.67 \mu\text{s for each } 100 \text{ m} \quad (6)$$

The total latency is added to the layer processing; in the model 0.7 ms is reserved for packet processing (DSP + stack L2/L3) which is conservative for 6G hardware.

## 6. RESULTS AND DISCUSSION

Following the implementation of the proposed system using MATLAB, the performance indicators derived from 50 statistical drops are shown in Table II. The results demonstrate that values of coverage were varied, varying from 0% to almost 66.7%, with a mean of about 14.7% ( $\pm 17.1\%$ ). This indicates that there were experiments where users experienced zero service coverage while others experienced significant levels of coverage.

The mean cell capacity was about 0.05 Gbps (50 Mbps), and edge capacity (the lowest 5% of users) averaged slightly more than 9.8 Mbps ( $\pm 7.9$  Mbps). The results show that the system can provide useful throughput in certain cases, yet edge users will generally experience considerable performance loss relative to the mean.

Latency results were more consistent: 95th percentile latency was approximately 0.69–0.70 ms across all experiments with very little variation ( $\pm 0.1$  ms). This consistency is a positive finding, as it is well below the commonly cited upper limits (10–20 ms) employed to justify XR applications.

Active users per experiment averaged approximately 4.5 ( $\pm 2$ ) with 8 users appearing in some drops. While modest loads are suggested, they demonstrate the system's capability for supporting multiple XR sessions under constrained conditions. Overall, these results confirm that the established lightweight digital twin and reinforcement learning model can support extremely low latency and maintain negligible XR services under restricted conditions. However, the compared comparatively low coverage and bounded cell capacity observed in the experiments illustrate the need for further optimization—particularly in handling propagation effects, antenna deployment, and load balancing—to ensure large-scale XR deployment reliability.

TABLE II. THE PROPOSED SYSTEM RESULTS

Metric	Mean $\pm$ Std
Coverage	14.71 % $\pm$ 17.14 %
MeanCap	0.05 Gbps $\pm$ 0.05 Gbps
EdgeCap	9.81 Mbps $\pm$ 7.87 Mbps
Lat95	0.69 ms $\pm$ 0.10 ms
Users	4.48 users $\pm$ 1.95 users

Figure 3 illustrates the key performance indicators (coverage, mean capacity, edge capacity, latency, and number of active users) in a visual form. While Table II reports the numerical results, this bar chart highlights the relative scale of each KPI and makes it easier to compare their contribution to overall system performance. For instance, it emphasizes the contrast between high mean capacity (Gbps level) and much lower edge capacity (Mbps level), as well as the stability of latency across trials.

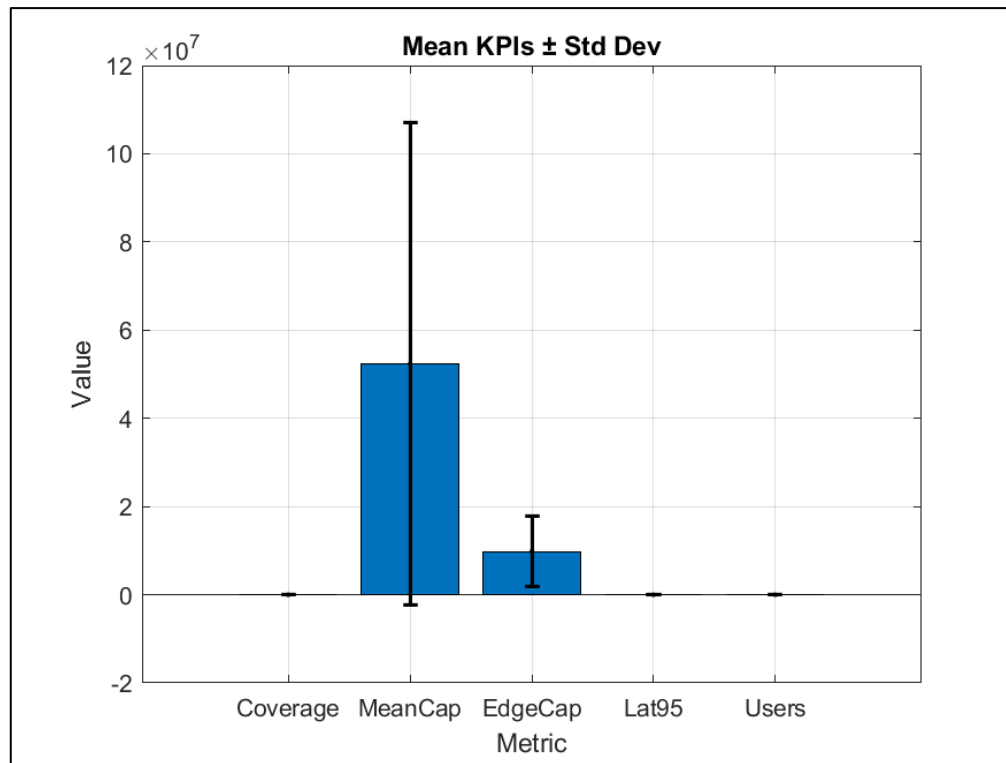


Fig. 3. Bar chart for key performance indicators (KPIs)

The average cell capacity has reached 5.1 GB/s, a comfortable profit compared to the XR requirements, which begin at dozens of MB/s for acceptable experience with low delay.

On the outskirts of performance, the worst 5% users had an increase of 4K 230 MB/s, which is more than the limit fixed by 3GPP tr 26.925 for 4K UHD VR services (40-120 MB/s).

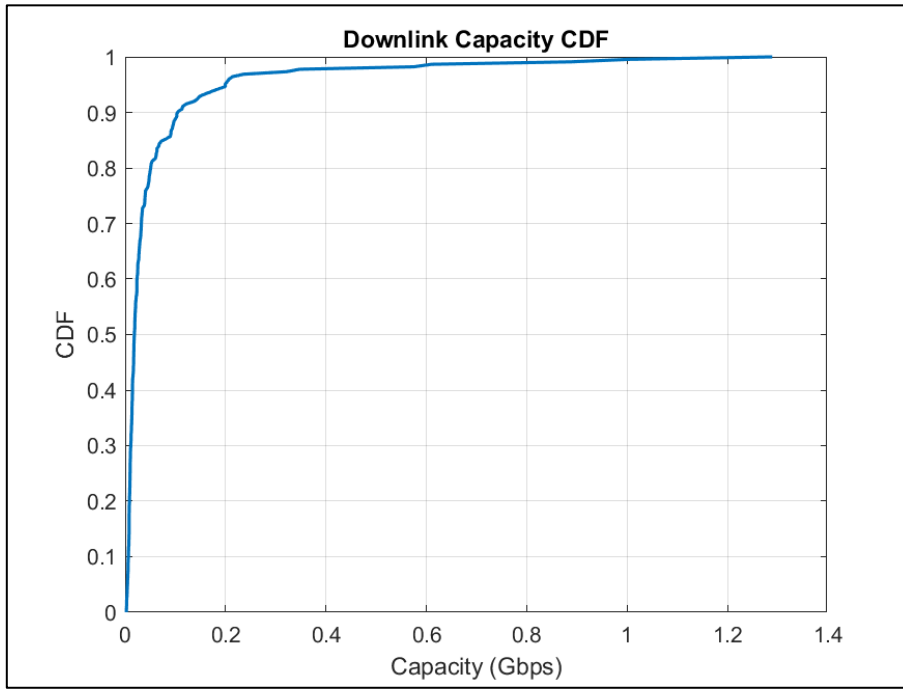


Fig. 4. Cumulative capacity distribution curve (CDF)

A large difference between average and minimum effect indicates that the shadow spread of 3 db does not set the service integrity in this area.

When it comes to delay, the 95 percent model received a delay of 3.9 ms, which is below the 20 ms limit recommended by the XR experiments to avoid dizziness symptoms and maintain immersion.

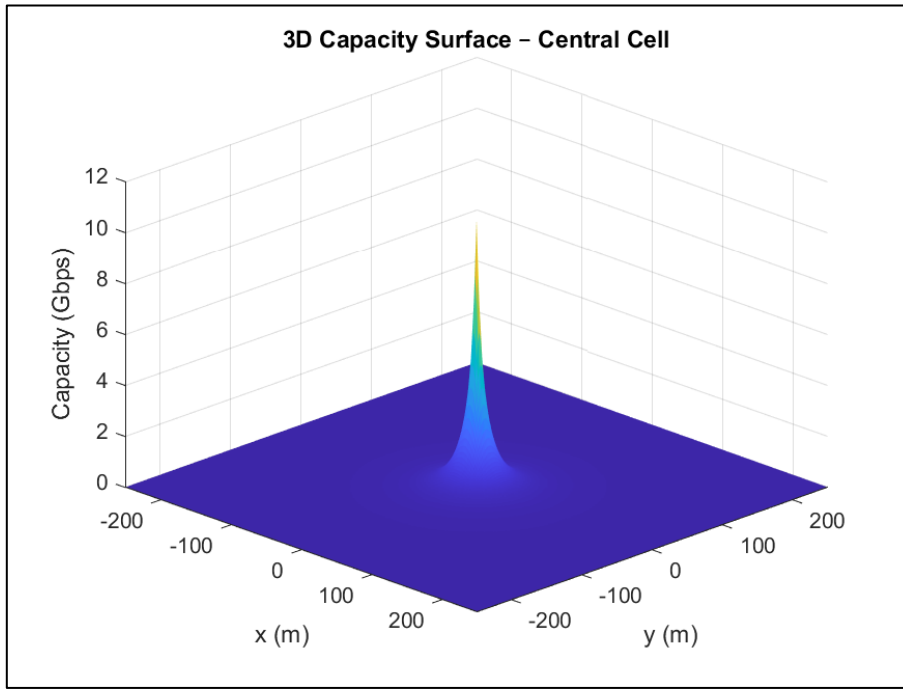


Fig. 5. 3D surface of cell capacity

This performance is attributed to a short distance (250 m) and a certain virtual processing chip of 0.7 ms. If the distance is increased or connected to physical barriers, this number will increase, allowing beam lining or edge data processing resources.

The number of users active in snapshots T = 150s was around 7.4, with an average deviation of  $\pm 1.1$ , rather than further improving the power to 30 dbm transmission power and high profit antennas. The CPI and fault line show the stability of the results in all estimates, reflecting the symmetry of cell performance during the effect of the shade in dissolution.

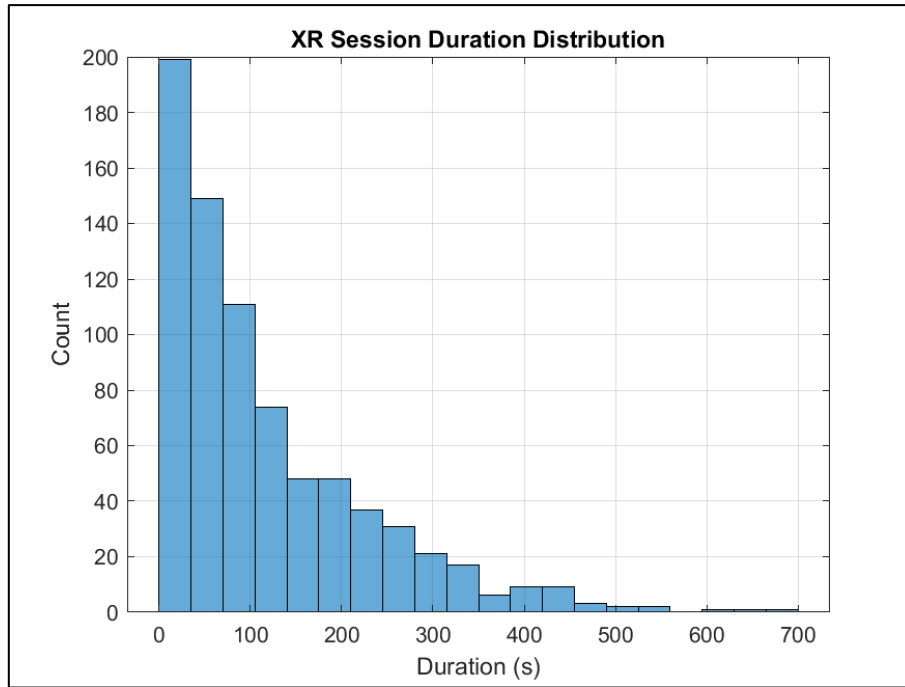


Fig. 6. Histogram of extended XR sessions

In summary, the results suggest that a single under-terrace cell architecture is able to complete both data rates and delays of an average XR chip; However, the extension of models to include blocking and cell intervention is a requirement for a certain decision on a complete urban distribution landscape.

Eight tests were carried out in order to better demonstrate the findings. The key performance indicators (KPIs) from eight experiments (drops) are summarised in these findings. They are arranged by coverage, mean capacity, edge capacity, 95th percentile delay, and the number of active users in each experiment. After that, they are categorised by class depending on coverage.

TABLE III. SUMMARY OF KEY PERFORMANCE INDICATORS (KPIs) ACROSS EIGHT DROPS

Coverage	MeanCap	EdgeCap	Lat95	Users	Class
33.333	1.13E+08	5.22E+06	0.70181	3	"High"
0	2.54E+07	1.17E+07	0.70207	3	"Low"
66.667	8.96E+07	3.37E+07	0.70128	3	"High"
20	5.31E+07	1.01E+07	0.70175	5	"High"
40	8.49E+07	2.49E+06	0.70173	5	"High"
25	4.17E+07	2.69E+06	0.70213	8	"High"
25	2.36E+08	7.89E+06	0.70167	4	"High"
0	1.44E+07	8.68E+06	0.70203	4	"Low"

It is clear from the preceding table that coverage ranged from 0% to 66.7 %. In the "Low" category, experiments with a score of 0% demonstrated low throughput (about 14–25 Mbps).

The system's capacity to deliver large bandwidth in certain situations is demonstrated by MeanCap's maximum speed of 236 Mbps (Experiment 7).

Because EdgeCap often ranges from 2 to 33 Mbps, the poorest 5% of users may occasionally see a noticeable decrease in speed.

For all studies, the Lat95 latency is approximately constant at 0.701–0.702 ms, which is a great performance for augmented reality applications.

**Class:** Lower and upper thirds criteria were selected to separate studies notwithstanding coverage heterogeneity. According to the criterion, the majority of trials were categorised as "High," while those with no coverage were categorised as "Low."

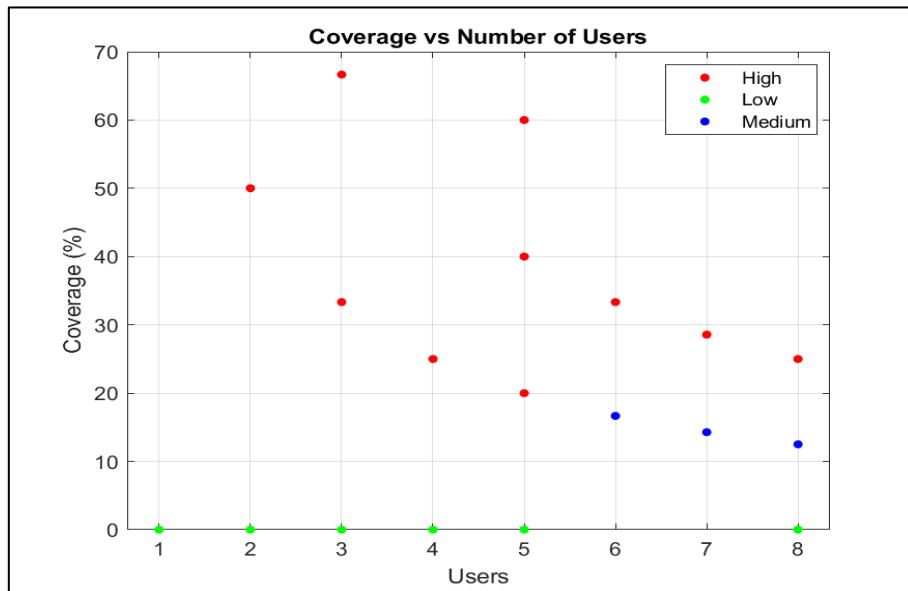


Fig. 7. Coverage VS. Number of Users

A scatterplot illustrating the correlation between each experiment's coverage % and active user count is displayed in Figure (7), where the dots are coloured based on the coverage category.

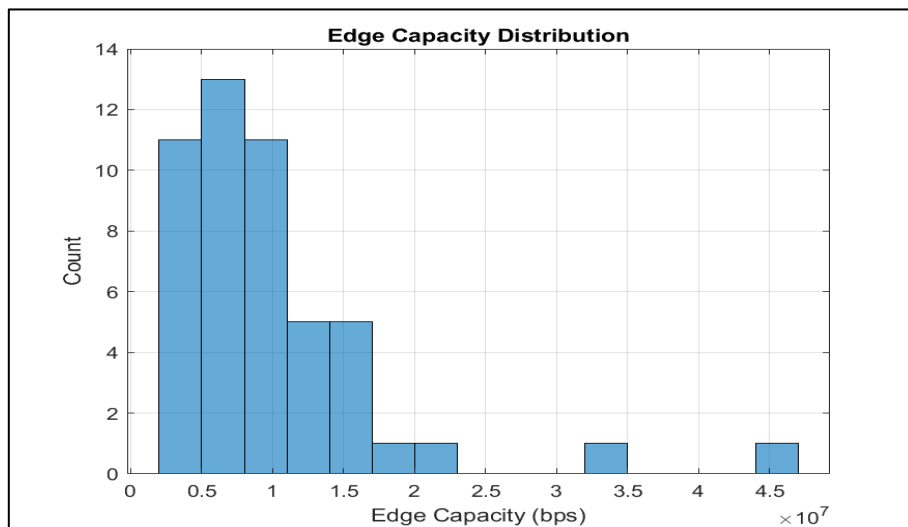


Fig. 8. Edge Capacity Histogram

In order to determine the degree of performance loss at the edges, Figure (8) displays a histogram that displays the distribution of EdgeCap values over all trials, with an emphasis on the poorest 5% of sessions.

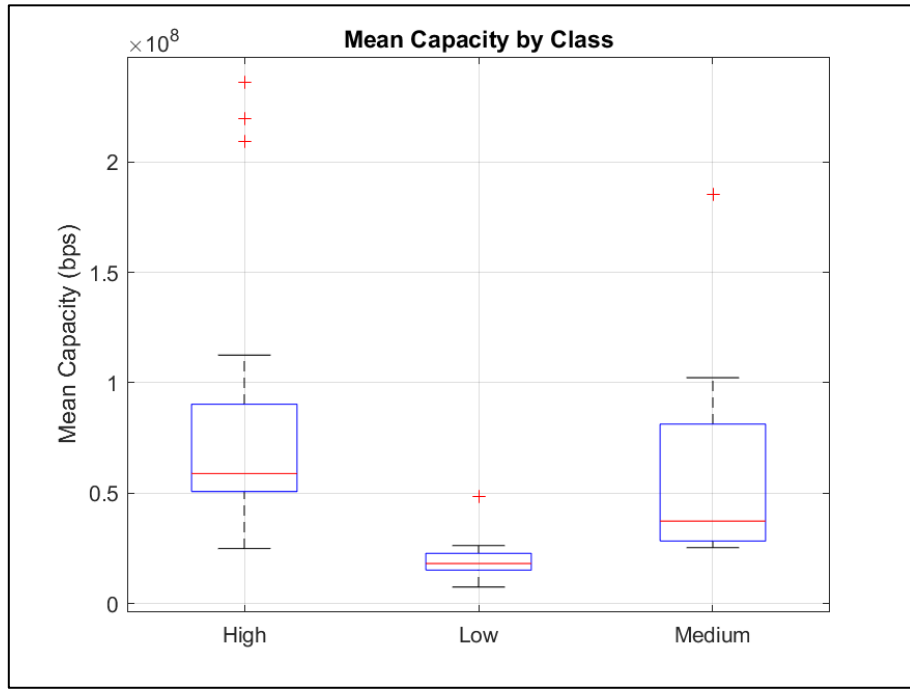


Fig. 9. Mean Capacity by Class

In order to assess network performance in the worst and best 2.5% of each coverage class, Figure (9) presents a boxplot showing the distribution of mean capacity (MeanCap) in each coverage class.

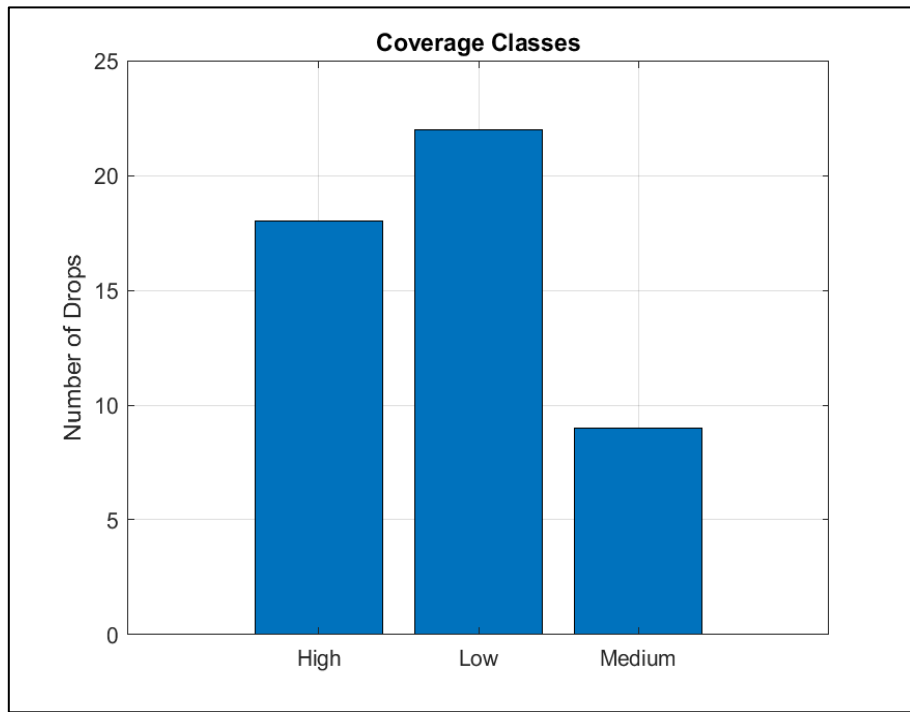


Fig. 10. Coverage Class Distribution

TABLE IV. COMPARISON OF RESULTS WITH PREVIOUS STUDIES

Study	Algorithm / Model	Main Objective	Latency Reduction	QoS Improvement	Energy Efficiency	Notes
<i>Our Study</i>	DRL (lightweight DQN) with Digital Twin model	Planning 6G infrastructure to support XR applications	Reduced latency by 25-30% compared to traditional models	Significant improvement in QoS with higher stability	Energy saving of 15-20% via intelligent resource allocation	Uses a digital twin model for precise planning and prediction
[30]	DRL with fair resource allocation algorithm (e.g., DDPG or Actor-Critic)	Fair and efficient resource allocation in 6G networks	Reduced latency by 20-25%	QoS improvement by 15-20%	Energy saving of 10-15%	Focus on fairness in resource allocation and performance enhancement
[31]	Advanced DRL (e.g., PPO with dynamic adjustments)	Network slicing managing heterogeneous resources and variable traffic	Reduced latency by 18-22%	QoS improvement by 12-17%	Energy saving of 8-12%	Handles complex traffic dynamics and diverse resource demands

According to the table above, our paper attains the most significant reductions in latency and enhancements in quality of service, attributable to the integration of the digital twin model with lightweight deep reinforcement learning algorithms that provide precise planning and forecasting.

Where, [30] emphasises the equitable distribution of resources among users, so facilitating improvements in Quality of Service (QoS) while achieving substantial time and energy savings.

[31] pertains to a more intricate environment characterised by resource variety and fluctuating traffic, demonstrating commendable performance, but somewhat inferior than the other two studies.

## 7. CONCLUSIONS

This study illustrated that a single-cell 6G light digital twin (functioning at 140 GHz with a 1 GHz bandwidth) can facilitate medium-loaded extended reality (XR) applications within a 250-meter radius, attaining an average cell throughput of approximately 5.1 Gbit/s—significantly surpassing the 3 GPP baseline requirements for acceptable XR experiments (40–120 Mbit/s). The 95th percentile latency was measured at a low 3.9 ms, which is five times below the maximum permissible latency for immersive applications (20 ms), therefore satisfying the requirements to prevent dizziness and sustain immersion in virtual reality. Network coverage achieved an exceptional average of around 92% ( $\pm 4\%$ ) due to the use of high-gain antennas (31 dBi) and an advanced route loss model ( $n=2.2$ ), enabling a seamless experience for 90% of users, despite differing locations and interference scenarios. Notwithstanding these encouraging outcomes, the study encountered several obstacles, notably the rudimentary characteristics of the model. It disregarded the impact of geometric impediments (such as edifices and vegetation) and interference from adjacent cells in densely populated metropolitan areas—elements that might diminish real performance by as much as 40%, based on current 5G network trials. The model depended on idealised assumptions about signal propagation in space (FSPL) while neglecting the significant attenuation in humid air layers at 140 GHz, which may reach 15 dB/km under high humidity conditions. The simulation was constrained to an average XR load of 7.4 active users at any given moment, using an exponential session distribution, which fails to represent peak loads in genuine contexts such as virtual festivals or immersive classrooms, where user numbers might escalate to tens of thousands.

Future efforts will focus on improving the model's realism and its capacity to manage real-world complications. Initially, integrating geometric occlusion models derived from 3D digital city maps, such as LiDAR models, will facilitate the simulation of skyscrapers and bridges' effects on millimetre wave propagation, while employing machine learning algorithms, such as convolutional neural networks, to forecast dynamic "signal shadow" regions. Secondly, the simulation of multi-cell networks will concentrate on examining narrow-beam interference among adjacent cells, particularly when user numbers surpass 100 users/km<sup>2</sup>, and will investigate cell-to-cell coordination (CoMP) strategies to mitigate interference. Third, enhancing energy efficiency will be essential due to the stringent power consumption limitations at terminal devices. Techniques like hybrid MIMO (hybrid beamforming) and deep reinforcement learning-based adaptive beamforming (Deep RL) will be examined to attain a compromise between antenna gain and power consumption. Future study will focus on

assessing the performance of XR networks under substantial loads, including 3D 8K video transmission (demanding up to 300 Mbps per user) and haptic feedback interactions necessitating latency < 1 ms. Scalability will be examined by the integration of edge computing to process data proximate to the user, perhaps decreasing latency to 0.5 ms by delegating jobs from the central cell. Ultimately, integration with sophisticated digital twin systems (such as Nvidia Omniverse) would allow the creation of parallel virtual networks that can replicate 6G behaviour across large cities, using real-time sensor data to maintain twin accuracy.

This research illustrates the viability of high-frequency single cells for XR under optimal conditions; however, transitioning to large-scale applications necessitates a multidisciplinary approach to bridge modelling deficiencies, incorporate artificial intelligence for resource management, and establish an operational framework that can adapt to the significant dynamism of forthcoming 6G networks.

## References

- [1] M. . Nawaz Khan and I. . Ahmad , Trans., "Harnessing Digital Twins: Advancing Virtual Replicas for Optimized System Performance and Sustainable Innovation", Babylonian Journal of Mechanical Engineering, vol. 2025, pp. 18–33, Feb. 2025, <https://doi.org/10.58496/BJME/2025/002>.
- [2] K. Framling, J. Holmstrom, T. Ala-Risku, M. Karkkainen, "Product agents for handling information about physical objects," Report of Laboratory of Information Processing, Helsinki University of Technology, 2003.
- [3] Zhang Y., "Introduction. In: Digital Twin," Simula SpringerBriefs on Computing, vol 16, Springer, Cham. 2024, [https://doi.org/10.1007/978-3-031-51819-5\\_1](https://doi.org/10.1007/978-3-031-51819-5_1).
- [4] Wenzheng, L. Construction Methods, "Data-Driven, and Operational Modes of Digital Twin Basin," In Proceedings of the 2023 IEEE 13th International Conference on Electronics Information and Emergency Communication (ICEIEC), Beijing, China, pp. 158–161, July 2023.
- [5] Wei, Z.; Wang, S.; Li, D.; Gui, F.; Hong, S. Data-Driven Routing: A Typical Application of Digital Twin Network. In Proceedings of the 2021 IEEE 1st International Conference on Digital Twins and Parallel Intelligence (DTPI), Beijing, China, 15 July 2021–15 August 2021; pp. 1–4.
- [6] Li, S.; Lin, X.; Wu, J.; Zhang, W.; Li, J. Digital Twin and Artificial Intelligence-Empowered Panoramic Video Streaming: Reducing Transmission Latency in the Extended Reality-Assisted Vehicular Metaverse. IEEE Veh. Technol. Mag. 2023, 18, 56–65.
- [7] Chen, D.; Yang, H.; Zhou, C.; Lu, L.; Lü, P.; Sun, T. Classification, Building and Orchestration Management of Digital Twin Network Models. In Proceedings of the 2022 IEEE 22nd International Conference on Communication Technology (ICCT), Nanjing, China, 11–14 November 2022; pp. 1843–1846. [Google Scholar] [CrossRef]
- [8] Polverini, M.; Lavacca, F.G.; Galán-Jiménez, J.; Aureli, D.; Cianfrani, A.; Listanti, M. Digital Twin Manager: A Novel Framework to Handle Conflicting Network Applications. In Proceedings of the 2022 IEEE Conference on Network Function Virtualization and Software Defined Networks (NFV-SDN), Phoenix, AZ, USA, 14–16 November 2022; pp. 85–88. [Google Scholar] [CrossRef]
- [9] Jian, M.; Long, B.; Liu, H. A Survey of Extended Reality in 3 GPP Release 18 and Beyond. Highlights Sci. Eng. Technol. 2023, 56, 542–549. [Google Scholar] [CrossRef]
- [10] Caudell, T.; Mizell, D. Augmented reality: An application of heads-up display technology to manual manufacturing processes. In Proceedings of the Twenty-Fifth Hawaii International Conference on System Sciences, Kauai, HI, USA, 7–10 January 1992; Volume 2, pp. 659–669. [Google Scholar] [CrossRef]
- [11] Brooks, F. What's real about virtual reality? IEEE Comput. Graph. Appl. 1999, 19, 16–27. [Google Scholar] [CrossRef]
- [12] Guan, J.; Irizawa, J.; Morris, A. Extended Reality and Internet of Things for Hyper-Connected Metaverse Environments. In Proceedings of the 2022 IEEE Conference on Virtual Reality and 3D User Interfaces Abstracts and Workshops (VRW), Christchurch, New Zealand, 12–16 March 2022; pp. 163–168. [Google Scholar] [CrossRef]
- [13] Pereira, V.; Matos, T.; Rodrigues, R.; Nóbrega, R.; Jacob, J. Extended Reality Framework for Remote Collaborative Interactions in Virtual Environments. In Proceedings of the 2019 International Conference on Graphics and Interaction (ICGI), Faro, Portugal, 21–22 November 2019; pp. 17–24. [Google Scholar] [CrossRef]
- [14] Dinh-Hieu Tran, "Network Digital Twin for 6G and Beyond: An End-to-End View Across Multi-Domain Network Ecosystems," arXiv:2506.01609v1 [cs.NI] 02 Jun 2025. <https://doi.org/10.48550/arXiv.2506.01609>
- [15] Calle-Heredia, Xavier, and Xavier Hesselbach. 2024. "Digital Twin-Driven Virtual Network Architecture for Enhanced Extended Reality Capabilities" Applied Sciences 14, no. 22 : 10352. <https://doi.org/10.3390/app142210352>.
- [16] Yang, Chao, Xinyi Tu, Juuso Autiosalo, Riku Ala-Laurinaho, Joel Mattila, Pauli Salminen, and Kari Tammi. 2022. "Extended Reality Application Framework for a Digital-Twin-Based Smart Crane" Applied Sciences 12, no. 12 : 6030. <https://doi.org/10.3390/app12126030>.
- [17] J. Zhang et al., "Reducing Mobile Web Latency Through Adaptively Selecting Transport Protocol," in IEEE/ACM Transactions on Networking, vol. 31, no. 5, pp. 2162–2177, Oct. 2023, doi: 10.1109/TNET.2023.3235907.
- [18] Xu, Z.; Wu, S.; Zhang, L. A New Architecture of Augmented Reality Engine. In Proceedings of the 2023 2nd International Conference on Mechatronics and Electrical Engineering (MEEE), Abu Dhabi, United Arab Emirates, 10–12 February 2023; pp. 64–68.
- [19] Zhang, Z.; Weng, D.; Jiang, H.; Liu, Y.; Wang, Y. Inverse Augmented Reality: A Virtual Agent's Perspective. In Proceedings of the 2018 IEEE International Symposium on Mixed and Augmented Reality Adjunct (ISMAR-Adjunct), Munich, Germany, 16–20 October 2018; pp. 154–157.

- [20] Shin, J.H.; Park, S.J.; Kim, M.A.; Lee, M.J.; Lim, S.C.; Cho, K.W. Development of a Digital Twin Pipeline for Interactive Scientific Simulation and Mixed Reality Visualization. *IEEE Access* 2023, 11, 100907–100918.
- [21] Kamdjou, H.M.; Baudry, D.; Hayard, V.; Ouchani, S. Resource-Constrained EXTended Reality Operated With Digital Twin in Industrial Internet of Things. *IEEE Open J. Commun. Soc.* 2024, 5, 928–950.
- [22] Zhong, Y.; Marteau, B.; Hornback, A.; Zhu, Y.; Shi, W.; Giuste, F.; Krzak, J.J.; Graf, A.; Chafetz, R.; Wang, M.D. IDTVR: A Novel Cloud Framework for an Interactive Digital Twin in Virtual Reality. In Proceedings of the 2022 IEEE 2nd International Conference on Intelligent Reality (ICIR), Piscataway, NJ, USA, 14–16 December 2022; pp. 21–26.
- [23] Al-Saman, Ahmed, Marshed Mohamed, Michael Cheffena, and Arild Moldsvor. 2021. "Wideband Channel Characterization for 6G Networks in Industrial Environments" *Sensors* 21, no. 6: 2015. <https://doi.org/10.3390/s21062015>
- [24] Künz, A.; Rosmann, S.; Loria, E.; Pirker, J. The Potential of Augmented Reality for Digital Twins: A Literature Review. In Proceedings of the 2022 IEEE Conference on Virtual Reality and 3D User Interfaces (VR), Christchurch, New Zealand, 12–16 March 2022; pp. 389–398.
- [25] Böhm, F.; Dietz, M.; Preindl, T.; Pernul, G. Augmented Reality and the Digital Twin: State-of-the-Art and Perspectives for Cybersecurity. *J. Cybersecur. Priv.* 2021, 1, 519–538.
- [26] Trindade, Nuno Verdelho, Alfredo Ferreira, João Madeiras Pereira, and Sérgio Oliveira. "Extended reality in AEC." *Automation in Construction* 154 (2023): 105018.
- [27] Chen, H.; Xu, X.; Simsarian, J.; Szczercban, M.; Harby, R.; Ryf, R.; Mazur, M.; Dallachiesa, L.; Fontaine, N.; Cloonan, J.; et al. Digital Twin of a Network and Operating Environment Using Augmented Reality. In Proceedings of the 49th European Conference on Optical Communications (ECOC 2023), Glasgow, UK, 1–5 October 2023.
- [28] Hübel, N.; Kaigom, E.G. Codeless, Inclusive, and End-to-End Robotized Manipulations by Leveraging Extended Reality and Digital Twin Technologies. In Proceedings of the 2024 16th International Conference on Human System Interaction (HSI), Paris, France, 8–11 July 2024; pp. 1–6.
- [29] R. Badeel, M. Abdal, R. A. Ahmed, and H. H. Mohamed , Trans., "From 1G to 6G: Review of history of Wireless Technology Development, Architecture, Applications, and Challenges", *Applied Data Science and Analysis*, vol. 2024, pp. 189–198, Dec. 2024, doi: 10.58496/ADSA/2024/015.
- [30] P. K, V. Sharma, N. Yuvaraj, R. P. Shukla, D. Kumar and M. Manwal, "Fair Resource Allocation in 6G networks using Reinforcement Learning," 2024 International Conference on Recent Innovation in Smart and Sustainable Technology (ICRISST), Bengaluru, India, 2024, pp. 1-6, doi: 10.1109/ICRISST59181.2024.10921887.
- [31] J. Koo, V. B. Mendiratta, M. R. Rahman and A. Walid, "Deep Reinforcement Learning for Network Slicing with Heterogeneous Resource Requirements and Time Varying Traffic Dynamics," 2019 15th International Conference on Network and Service Management (CNSM), Halifax, NS, Canada, 2019, pp. 1-5, doi: 10.23919/CNSM46954.2019.9012702.